Current Science
CS 5 (2), 2098-2108 (2025)
Received 10 Feb 2025 | **Revised 17 March** 2025 | **Accepted 15 April**. 2025 | **Online Available 30 April** 2025
https://doi.org/ 10.52845/CS/2025-5-2-65

Current Science

Current Science

OPEN ACCESS

ISSN(O)2795-8639

Research Article

In Vivo Study of GFT-505 Selenium-Substituted Derivatives for the Treatment of Metabolic Dysfunction-Associated Steatohepatitis

JiaWen Wang[a], Mengzhen Yuan[a], Yi Zou[a], Yue Yu[b], JiaJia Yu[a], Jiang Liu[a], Peng Yu[a], Zhen Liu[a], Cen Xiang[a,*], Yuou Teng[a,*]

[a] China International Science and Technology Cooperation Base of Food Nutrition/Safety and Medicinal Chemistry, State Key Laboratory of Food Nutrition and Safety, Tianjin University of Science and Technology, Tianjin, 300457, China.

[b]Deji Pharmaceutical Technology (Tianjin) Co., Ltd

[*]Corresponding Author: Cen Xiang, Yuou Teng

Abstract:
Metabolic dysfunction-associated steatohepatitis（MASH） is a common liver disease worldwide and can develop into liver cirrhosis and liver cancer. Current treatment is limited, and the only drug Rezdiffra has limited effects. GFT-505 performed well as a PPAR agonist in stage II, but not as expected in stage III. We replaced the sulfur atom of GFT-505 with selenium to obtain compound 4c. Study evaluating the effect of 4c on the MASH mouse model induced by MCD. The results showed that 4c improved MASH through multi-target synergy and reduced TG and ALT better than GFT-505. This finding provides a theoretical basis and new ideas for the development of novel multi-target anti-MASH drugs.

Keywords：**MASH, GFT-505, Selenium, PPAR, Proteomics**

Introduction

Metabolic dysfunction-associated fatty liver disease (MAFLD) is idiopathic hepatic steatosis confirmed by imaging or histology in the absence of secondary causes of hepatic fat accumulation such as alcohol, drugs and viruses, which is the most common causes of chronic liver disease[1-2]. The prevalence of MAFLD is estimated to be 25-34% in developed countries and 29.2% in China, affecting about a quarter of the world's population[3-5]. If MAFLD is not treated in time, MAFLD will develop into MASH. MASH is a progressive MAFLD, about 20%-27% of MAFLD patients will develop MASH, and over time it can develop into cirrhosis and even hepatocellular carcinoma, and MASH is the fastest growing cause of hepatocellular carcinoma. Further increase the health and economic burden[6-7]. The current treatment methods of MAFLD include external factor therapy, drug therapy and surgical treatment[8-9]. Healthy diet is the most basic treatment method, and drug treatment generally has a safety problem. Surgical treatment is the current effective treatment method, but it is accompanied by severe fibrosis after surgery[10-12]. At present, Rezdiffra is the only marketed drug for MASH, but the disease mechanism of MASH is complex, and a single target drug cannot deal with the whole MASH market[13-14].

GFT-505 is a PPAR modulator that exhibits preferential activity against PPAR δ and concomitant activity against PPARα. Peroxisome proliferator-activated receptors (PPAR), a member of the nuclear hormone receptor superfamily, are a class of transcription factors activated by ligands[15-16]. PPAR contains three isoforms, α, β/δ and γ, which are expressed in different tissues and participate in a variety of physiological processes such as energy metabolism, fatty acid transport and inflammatory response in the body[17-20]. The success of clinical studies on PPAR agonists has stimulated the development of more new products, such as

selective PPARβ/δ activators, dual PPAR agonists and pan-PPAR agonists[21]. Phase II clinical data of **GFT-505** suggest that it may be an effective agent for the treatment of MAFLD/MASH associated with the metabolic syndrome[22-24]. However, its phase III clinical data (ClinicalTrials.gov number:NCT02704403) are not ideal, and it can not effectively improve MASH and inhibit liver fibrosis, so that **GFT-505** failed to reach the clinical endpoint[25-26].

Selenium metal is a material with unique chemical properties that has attracted much attention in the field of drug research and development in recent years. The introduction of metal selenium can not only change the chemical structure of compounds, but also significantly improve their pharmacological activities, especially in cancer treatment, anti-inflammation and anti-oxidation[27-28]. The polarization effect of selenium atoms makes it easier for compounds to be identified and act *in vivo*[29-30].With the deepening of research, selenium metal will have a broader application prospect in the field of medicine.

Our research group has synthesized a series of derivative compounds targeting **GFT-505** in the early stage, as shown in Figure S1, through structural modification to improve its drug activity, Among them, compound 3d obtained by replacing the sulfur atom of **GFT-505** with imine and replacing its carboxyl terminal with tert-butyl ester and compound **4c** obtained by replacing the sulfur atom of **GFT-505** with metal selenium showed good anti-MASH drug activity *in vitro*. Further, 3d was used as the lead compound to test its anti-MASH drug activity *in vivo*. It shows a good anti-MASH effect *in vivo*. [31] In this study, we will further study the activity of compound **4c**. The target of its action was investigated, and the *in vivo* activity was evaluated using MCD-induced MASH model, and the mechanism of its action was investigated.

2 Result and Discusstion

2.1 Effects of GFT505 and 4c on Liver Histopathology in MCD-induced MASH Mice

Pathological changes in the liver are shown in Figure 1A. In the blank group, the liver tissue had regular structure, complete hepatocyte morphology, uniform cytoplasm, regular, round nucleus, located in the center of the cells, without pathological changes. In the model group, hepatocytes were disorganized, with nuclear fragmentation, vacuolar degeneration and intracellular lipid aggregation. The fenofibrate group, but still showed small amounts of lipid accumulation. Compared with fenofibrate**, GFT-505** and 4**c** at the same dose (3 mg/kg) had less fat vacuoles and less lipid accumulation. The pathological section of the high dose (30 mg/kg) **4c** was basically the same as the blank group, the vacuolar degeneration disappeared, the liver tissue structure was regular, and the hepatocytes returned to an intact state. The change of TG content in the liver also confirmed the results of H&E staining, as shown in Figure 1B, **GFT-505** and **4c** reduced the lipid content in the MASH model, but it is noteworthy that selenium-replaced 4c significantly increased the drug activity compared to **GFT-505** (p <0.05).The TG content of **GFT-505** (3 mg/kg) was 20.63 mg/g, **4c** 3 mg/kg, 10 mg/kg, and the TG content of 30 mg/kg were 11.89,11.45 and 11.77 mg/g, respectively.

The liver index is used in animal experiments to assess conditions such as nutritional status, disease progression or drug response, usually described by measuring the weight of the liver relative to the weight of the animal[31-32]. Compared with the blank and model groups, as shown in Figure 1C, the liver index was 5.3% **for GFT-505**, and **4c** was 4.1% at low doses, significantly different from the blank group (p <0.05). Notably, at the same dose, 4c was less liver toxic at lower doses than **GFT-505**, with a significant difference between **4c** and **GFT-505**, suggesting that 4c is less hepatotoxic than **GFT-505**.

These results indicate that, although **GFT-505** and **4c** induce hepatotoxicity, GFT-505 is more hepatotoxic than **4c**. This is mutually verified with previous *in vitro* cytotoxicity experiments and is consistent with the results of cellular experiments [33].

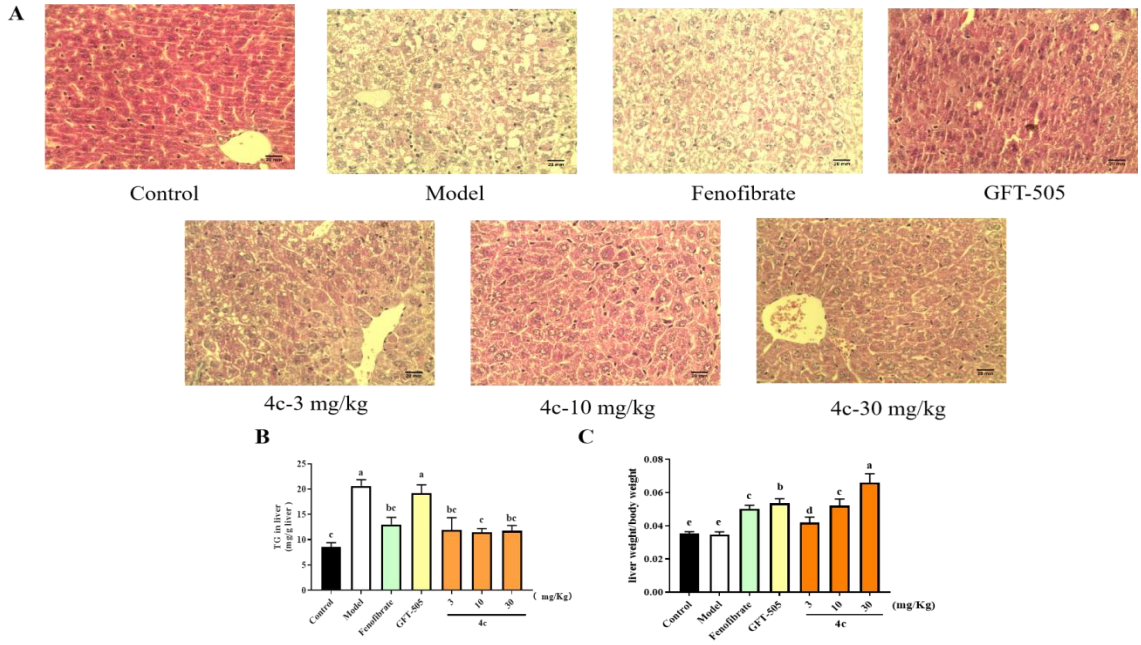

Figure.1. Effects of GFT-505 and 4c on liver histopathology in MCD-induced MASH mice. (A)H&E staining of MASH mice in the presence of GFT-505 and 4c (400×). (B) Effects of GFT-505 and 4c on liver TG in MASH mice. (C) Effects of GFT-505 and 4c on hepatotoxicity in MASH mice.All compounds at different concentrations were administered to mice for 4 weeks. Different letters indicate $p< 0.05$.

2.2 Effects of GFT-505 and 4c on physiological and biochemical parameters in MCD-induced MASH models.

In the context of MASH, hepatic steatosis is primarily attributed to the excessive accumulation of TG within hepatocytes. This condition arises when the liver's capacity to metabolize and export TG is overwhelmed by its rate of synthesis, leading to a significant increase in intracellular TG levels. Consequently, TG has emerged as a pivotal biomarker for the detection and assessment of MASH, reflecting the extent of lipid accumulation in the liver[34-36]. ALT and AST serve as crucial biochemical indicators for the verification of liver injury. In patients with MASH, elevated levels of ALT and AST are frequently observed, often correlating with the severity of the inflammatory response within the liver. The reduction of ALT and AST levels is thus regarded as a primary therapeutic objective in the management of MASH, reflecting the mitigation of hepatocellular injury and inflammation[37]. High-density lipoprotein (HDL) can transport free cholesterol to the liver and enter bile or bile acids, which has an anti-atherogenic effect and enhances the ability of blood lipid metabolism. MASH patients usually have low HDL[38-40].

Compared with **GFT-505**, compound **4c** had significantly increased efficacy in reducing TG, AST and ALT, whereas its ability could be comparable to that of **GFT-505** in reducing TC and improving HDL. The specific results are shown in Figure Figure 2A-2E. Compared with **GFT-505**,**4c** low dose (3 mg/kg) was more potent to lower TG content than **GFT-505**. Serum TG levels were 0.61 in the **4c** low-dose, **GFT-505**, and fenofibrate, 0.79, and 0.67 mmol/L groups, respectively (p <0.05).It is noteworthy that although **4c** has the ability to reduce serum TC content compared to the model group (Figure 2B), its ability to reduce TC was not as effective as **GFT-505**. Serum TC level, model group, **GFT-505** and **4c** were 2.57,6.69,4.34 and 5.46 mmol/L, respectively (p <0.05), indicating that although **4c** affected the total cholesterol level to some extent, its main effect was still to reduce the triglyceride content. Probably because **4c** is involved in specific pathways regulating lipid metabolism that selectively affect the levels of triglycerides and, to a lesser extent, the level of total cholesterol[41].The effects of **4c** and **GFT-505** on HDL are shown in the results of Figure 2C, showing increased HDL content with **GFT-505** and **4c** compared to the model group. At the same dose, the HDL protein

content was similar in the two groups. Serum HDL levels were 1.88,0.32,0.83, and 0.45 mmol/L in the blank, model, **GFT-505**, and **4c** groups, respectively (p <0.05). Compared with **GFT-505**,**4c** was significantly higher in reducing ALT and AST than was **GFT-505**. Serum ALT levels in blank, model, **GFT-505** and **4c** were 44.54,184.43,218.88,119.2U/L (p <0.05), which effectively reduced liver injury (Figure 2D-2E). In conclusion, **4c** can significantly reduce liver inflammation while significantly reducing TG content compared with **GFT-505**.

TNF-α, IL-6, and IL-8 are a range of proinflammatory factors. Of endotoxin-induced liver injury in patients with MASH. Endotoxin activates hepatic Kupffer cells and promotes the release of inflammatory cytokines to mediate the inflammatory response in MASH[42]. 4c the ability to reduce TNF- α and IL-6 is stronger than GFT-505, while the ability to reduce IL-8 is similar to **GFT-505**. As shown in Figure 2F, the ability of **4c** to reduce TNF- α at the same dose (3 mg/kg) was stronger than GFT-505, with significant differences. Specifically, the serum TNF- α level was 17.28 ng/L, 372.32 ng/L in the model group, and **GFT-505** and **4c** were 348.47 ng/L and 309.67 ng/L, respectively (p <0.05).Figure 2G shows that IL-8 is significantly lower in **GFT-505** and **4c** as compared to the model group. The serum IL-8 content was 65.53 ng/L in the blank group and 303.78 ng/L in the model group. At the same dose (3 mg/kg), the serum IL-8 levels of **GFT-505** and **4c** were approximately 230 ng/L (p <0.05). Figure 2H shows that both **GFT-505** and **4c** significantly reduced the content of IL-6, but **4c** significantly had more ability to reduce serum IL-6 than **GFT-505.** Serum IL-6 content was 12.15 ng/L in the blank group and 272.85 ng/L in the model group. The serum IL-6 levels of GFT-505 and 4c were 212.18 ng/L and 138.77 ng/L, respectively (p <0.05).

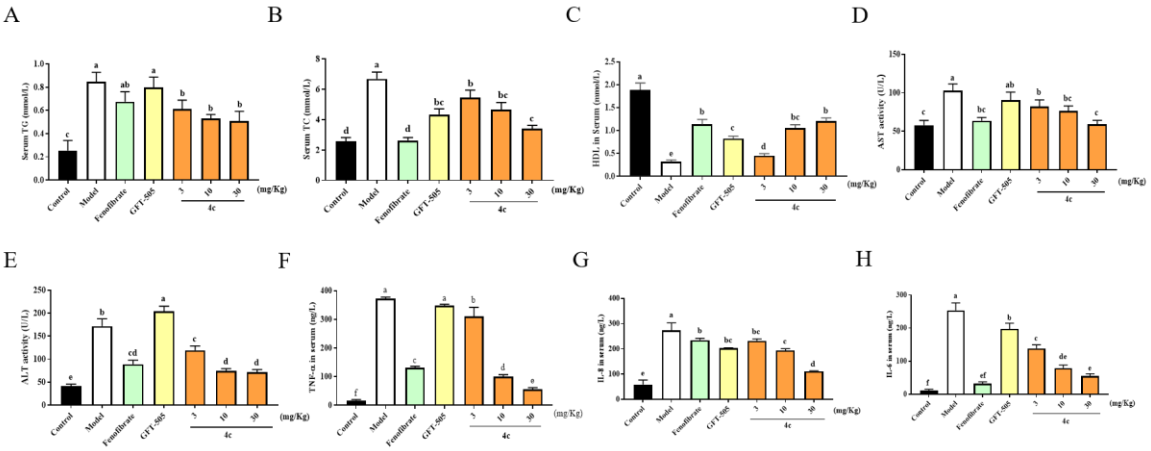

Figure.2. Effects of GFT-505 and 4c on physiological and biochemical parameters in MCD-induced MASH models.
Effect on TG(A), TC(B), HDL(C), AST(D), ALT(E), TNF-α(F), IL-8(G), IL-6(H) content in serum. Different letters indicate p< 0.05.

2.3 Differential Protein Analysis in Mice Samples.

Screening differential proteins can identify proteins whose expression levels change in different conditions or tissues, providing insight into biological processes and disease mechanisms in organisms[43]. Compared with the model group, the number of differentially expressed proteins changed after treatment with **4c** (Figure 3A, S2). These results indicate that **4c** can regulate the protein expression in mice, reduce the abnormal protein expression in the disease state, and thus may play a role in improving the disease state. Reactome can provide insight into underlying biological processes and identify potential biomarkers or therapeutic targets. The results are shown in Figure S3, which may affect the transport process of peroxisome proteins and the oxidation process of long-chain fatty acids.

To further investigate the possible functions and pathways regulated by **4c**, GO and KEGG analyses were performed. Three parts, biological

process (BP), cellular component (CC), and molecular function (MF), were examined, and the results are shown in the figure. In BP, enrichment results showed that **4c** may regulate REDOX processes, fatty acid oxidation and fatty acid metabolism (Figure 3B). In CC, **4c** mainly affected the composition of the membrane, endoplasmic reticulum, peroxisomes, etc. (Figure S4). In MF, **4c** may affect oxidoreductase activity, iron binding, and heme binding (Figure S5). KEGG enrichment results showed that **4c** may be involved in peroxisome pathway and PPAR signaling pathway (Figure 3C-3D,S6). These results suggest that **4c** may regulate MASH by fatty acid metabolism through fatty acid oxidation in peroxisomes, and the experimental results are consistent with the Reactome results.

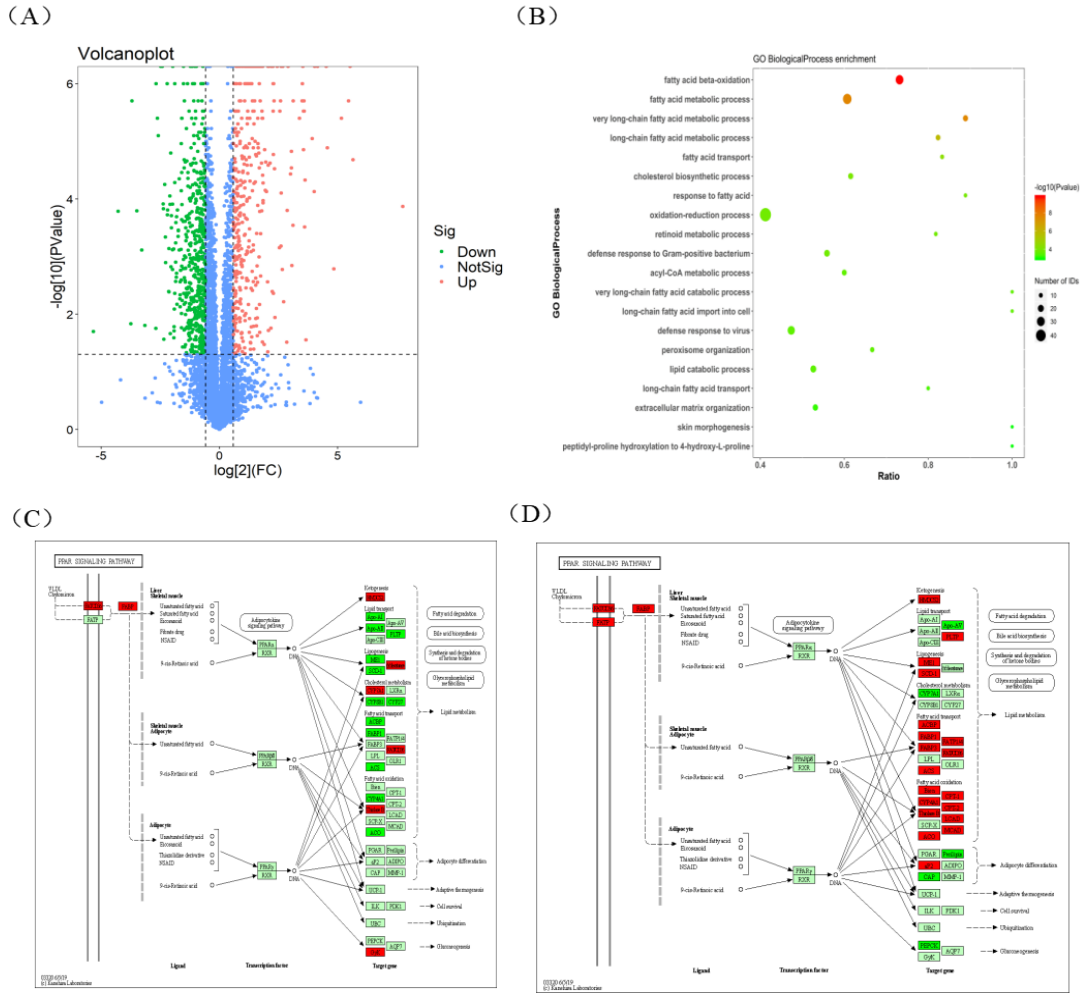

Figure.3. Differential protein analysis in mice samples.
(A) Analysis of the 4c differential protein.(B) BP protein annotation analysis of samples in 4c liver tissue. KEGG analysis of PPAR pathways in (C) model group and (D) 4c compound.

2.4 Protein Analysis of Key Genes in the PPAR Pathway.

In order to further verify the mechanism of 4c in the treatment of MASH, we selected some key regulatory genes and proteins for mechanism verification by KEGG data analysis. Firstly, we compared the difference in RNA expression levels between **GFT-505** and **4c**. Results as shown in Figure 4A-4E, compared with the model group, **GFT-505** and **4c** could effectively up-regulate the upstream gene FATP1. The relative expression levels of FATP1 gene in the blank group, the model group, the **GFT-505** group and the **4c** group (10 μM) were 1, 0.4, 0.7 and 0.65, respectively ($p < 0.05$). FATP1 is a transmembrane protein that is mainly involved in the transport of fatty acids in animals. Overexpression of FATP1 can accelerate the transport of fatty acids and regulate important physiological processes such as maintaining energy balance, thermogenesis, and insulin

resistance in adipose and muscle tissues. **GFT-505** and **4c** can also regulate PPAR γ, PPAR α and PPAR δ. Notably, **GFT-505** is a dual activator of PPAR α and PPAR δ, and its substitution with selenium did not reduce the activity of dual activation. The relative expression levels of PPAR γ gene in HepG2 cells of blank group, model group, **GFT-505** group and **4c** group (10 μM) were 1, 0.75, 0.94 and 1, respectively (p < 0.05).PPAR γ can promote the β-oxidation of fatty acids, thereby reducing lipid accumulation in the liver.

Luciferase reporter gene also showed that **GFT-505** and **4c** had similar activities on the activation of PPAR δ, PPAR γ and PPAR α, as shown in Figure 4F-4H. Most importantly, 4c could significantly reduce the content of SCD1 compared with GFT-505. The relative expression levels of SCD1 gene in the blank group, model group, **GFT-505** and **4c** (10 μM) were 1, 1.4, 0.9 and 0.8, respectively (p < 0.05), as shown in Figure 4E. SCD1 depletion leads to increased AMPK activity, which in turn promotes fatty acid oxidation and reduces liver fat content. WB results also showed that compared with the model group, **4c** could effectively up-regulate FATP1 in the PPAR pathway, without changing the content of PPAR δ and PPAR α, but could up-regulate the content of PPAR γ and down-regulate the content of SCD1, affecting the DNL process and its downstream routes, as shown in Figure 4I-4N.

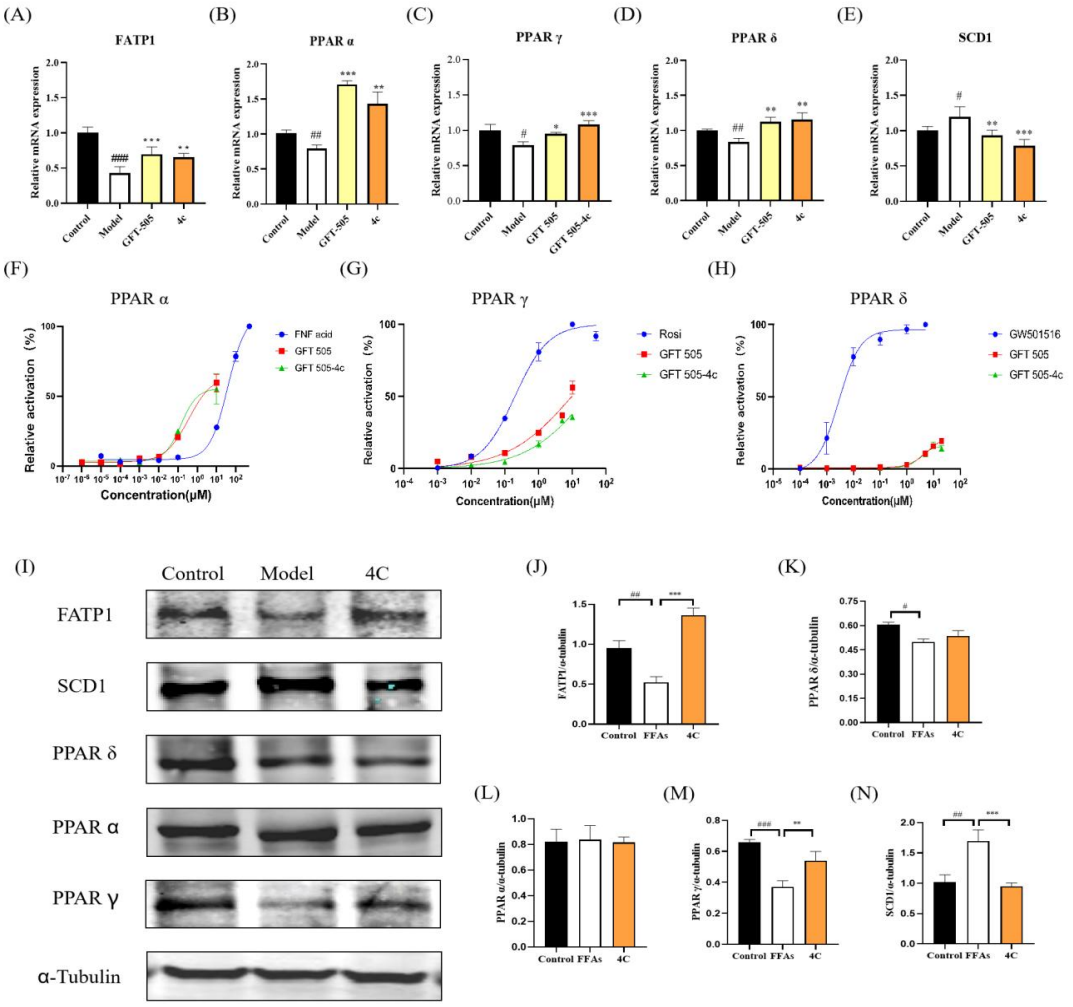

Figure.4. Protein analysis of key genes in the PPAR pathway.
Analysis of FATP1 (A), PPAR α (B), PPAR γ (C), PPAR δ (D), SCD1 (E) gene expression in different compounds of mice HepG2 cells. PPAR α (F), PPAR γ (G) , PPAR δ (H) activation as assessed by luciferase reporter assay. (I) Changes of key proteins in PPAR pathway in HepG2 cells of blank, model and 4c compound. (J) Gray scale analysis of FATP1 (J), PPAR δ (K), PPAR α (L), PPAR γ (M), SCD1 (N) protein in different groups.
Different letters indicate p< 0.05.

3 Conclusions

This study identified selenium-derivative **4c** as a promising MASH treatment. Both **4c** and GFT-505 improved liver pathology in mice, with **4c** showing lower hepatotoxicity at high doses. **4c** more effectively reduced TG, AST, ALT, and IL-6 than **GFT-505**. Mechanistic studies indicated 4c's influence on peroxisome and PPAR pathways, confirmed by qPCR and WB. 4c enhanced FATP1 and PPARγ expression, inhibited SCD1, and promoted fatty acid oxidation and transport, reducing fat content. Thus, **4c** is a potential MASH therapeutic.

4 Experimental

4.1 Animal Studies

C57BL/6J SPF male mice were purchased from Beijing Weitong Lihua Company and used to establish a high-fat model using the MCD(product number: TP3005R) method. The MCD and control MCS diets were custom-made by Nantong Talofei Feed Technology Co. Ninety mice were randomly divided into 9 groups, with 10 mice in each group. The control group was fed the MCS diet, while the remaining mice were fed the MCD diet for 4 weeks. Fenofibrate acid at 100 mg/kg and GFT-505 and 4c at 3 - 30 mg/kg were dissolved in 0.5% (M/V) carboxymethyl cellulose and administered orally daily for 4 weeks. The control group and the model group were also given 0.5% carboxymethyl cellulose solution orally daily for 4 weeks.

After 4 weeks, the orbital blood was collected into a 1.5 mL centrifuge tube, left at room temperature for 2 h, centrifuged at 2000 r/min for 10 min, and the supernatant (serum) was collected and stored in a refrigerator at -80 ℃ for later use. The mice were sacrificed by neck removal and the livers were dissected to calculate the liver index.

4.2 Liver H&E Staining

The liver tissue 0.5 cm from the edge of the right lobe of the liver was taken and fixed with neutral formalin solution. After dehydration, paraffin embedding, sectioning, H&E staining, and sealing, the pathological tissue sections were obtained, and then the pathological changes of liver tissues were observed under a light microscope. Pathological examination was performed using a three-eye inverted biomicroscope.

4.3 Liver Index and Biochemical Indexes Were Tested

The dissected liver was washed with pre-cooled normal saline, and the water on the surface of the liver was discarded. The liver index was calculated by weighing and recording with an electronic balance. The liver index was calculated using the formula shown in the formula.

Liver index (%) = liver mass/body mass*100%

Biochemical indicators such as TG, TC, AST, ALT, HDL, LDL, TNF-α, IL-6 and IL-8 in serum were detected according to the instructions of the kit. The kits of TG, TC, AST, ALT, HDL and LDL were all from Nanjing Jianxian Bioengineering Research Institute Co., LTD. The detection kits of TNF-α, IL-6 and IL-8 were from Nanjing Jiancheng Biological Company.

4.4 Differential Protein Analysis

A specific gene or protein was queried by the search function, and the biological pathways involved were browsed in the Pathway Browser. Enrichment Analysis of the list of candidate genes or proteins was performed using the Analysis Tool to identify significantly associated pathways. Finally, P and FDR values were calculated to assess the statistical significance of the results.

4.5 GO and KEGG Enrichment Analysis in Silico

Based on the identified protein ID, the mapping method was used to obtain the GO database annotation information of the proteins from the Uniprot database, and the functional classification of the proteins was annotated. For the GO nodes involved in BP, CC and MF, the numbers of all the corresponding proteins were listed, and the secondary classification of the expressed proteins was statistically plotted. Differentially expressed proteins were annotated against the KEGG database to determine the corresponding KEGG pathway for each protein. The functional enrichment of proteins in specific pathways was evaluated by comparing the significance of KEGG pathways between the experimental group and the control group.

4.6 RNA Extraction, cDNA Synthesis, and qPCR

Total RNA was extracted from HepG2 cells using Triquick Reagent (Solebo), and cDNA was

synthesized by reverse transcription from PrimeScriptTM FAST RT reagent Kit with gDNA Eraser (Takara). qPCR was performed using TB Green® Premix Ex TaqTM II FAST qPCR (TaKaRa) on a QuantStudio 1 Plus analyzer, and data were analyzed using QuantStudio 1 Plus software. GAPDH was used as an internal control, and relative mRNA expression differences were calculated using the 2-ΔΔCt method. The primer sequences were as follows.

Gene	Primer forward (5'-3')	Primer reverse (5'-3')
SCD1 (human)	CTCCTGGCTCGGGGTAAAAA	TAGAGGGGCATCGTCTCCAA
FATP1 (human)	GGACCCCAACGCGATATAC	GCCTCGTCTTCTGGATCTTG
DBI/ACBP (human)	CTCTAAAGGCGCTTGCCAGT	TATGTCGCCCACAGTTGCTT
PPAR α (human)	TCCTCGGTGACTTATCCTGT	GCGTGGACTCCGTAATGATAG
PPAR δ (human)	GCCTCTATCGTCAACAAGGAC	GCAATGAATAGGGCCAGGTC
PPAR γ (human)	GGGATCAGCTCCGTGGATCT	TGCACTTTGGTACTCTTGAAGTT
GAPDH (human)	ATGGGTGTGAACCATGAGAAG	GAGTCCTTCCACGATACCAAAG

4.7 PPAR Luciferase Reporter Assay

The 293T cells were seeded at a density of 6×10^4 per well in a 96-well plate and cultured for 24 hours at 37°C,5% CO_2. Transfection was performed using Lipofectamine 2000 according to the manufacturer's instructions. A total of 0.1 μg per well pBIND-PPARs, 0.1 μg per well pG5Luc, and 0.5 μl per well Lipofectamine 2000 were used to form DNA-liposome complexes. After transfection, different concentrations of test compounds or positive control drugs were added, followed by another 24-hour culture. Following cell lysis, luciferin from fireflies and sea kidneys was added, and the dual-luciferase signals were detected using a SYNERGY H1 plate reader. Data were normalized. The formula for calculating the activation percentage is as follows:

$$\text{activation\%} = \frac{X - X_{min}}{X_{max} - X_{min}} \times 100 (\text{X is the "F/R" of each concentration point} = \frac{\text{Firefly}}{\text{Renilla}}$$

X_{min} is the mean of blank values, and X_{max} is the mean of the maximum activation values of positive compounds)

The EC_{50} values of the test compounds were obtained using GraphPad 8 software.

4.8 Western Blot

Proteins were extracted from HepG2 cells and their concentration was determined using UV spectrophotometry. The protein samples were mixed with 6× SB buffer, boiled for 5 minutes, and then subjected to SDS-PAGE electrophoresis before transferring to PVDF membranes. The membrane was blocked with 5% (M/V) skim milk for 1 hour, followed by overnight incubation with the primary antibody at 4°C. After three washes, HRP-labeled secondary antibody was added, and Gel Doc™EZ Imager was used to visualize the bands. Finally, Western blot band intensity was semi-quantitatively analyzed using ImageJ software, with α-Tubulin as the reference.

4.9 Statistical Analysis

The data were expressed as the mean±standard deviation (SD). Statistical analysis was conducted using DPS v9.50 software, employing Duncan's new multiple range test for data processing and analysis. GraphPad Prism 8 software was utilized for additional analyses. Differences were considered statistically significant at $p < 0.05$.

Data Availability

The datasets examined and collected will be made available upon request and all supporting data for this study are also available in the ESI.

Conflicts of Interest

The authors declare no conflicts of interest.

Authorship Contribution Statement

JiaWen Wang: Data curation, Investigation and Methodology. **Mengzhen Yuan**: Writing – original draft, Investigation, Methodology and Formal analysis. **Yi Zou**: Validation and Visualization. **Yue Yu**: Methodology. **JiaJia Yu**: Methodology. **Jiang Liu**: Data curation and Formal analysis. **Zhen Liu**: Investigation. **Peng Yu**: Conceptualization and Writing – review & editing. **Cen Xiang**: Resources. **Yuou Teng**: Conceptualization, Project administration, Resources and Supervision.

References

1. Morrow, M. R. and Batchuluun, B. and Wu, J. and Ahmadi, E. and Leroux, J. M. and Mohammadi-Shemirani, P. and Desjardins, E. M. and Wang, Z. and Tsakiridis, E. E. and Lavoie, D. C. T. and Reihani, A. and Smith, B. K. and Kwiecien, J. M. and Lally, J. S. V. and Nero, T. L. and Parker, M. W. and Ask, K. and Scott, J. W. and Jiang, L. and Paré, G. and Pinkosky, S. L. and Steinberg, G. R., Inhibition of ATP-citrate lyase improves NASH, liver fibrosis, and dyslipidemia. *Cell Metabolism*, 2022, 34, 919-936.e918.
2. Chalasani, N. and Younossi, Z. and Lavine, J. E., The diagnosis and management of nonalcoholic fatty liver disease: Practice guidance from the American Association for the Study of Liver Diseases. *Clinical Liver Disease*, 2018, 11.
3. Younossi, Z. and Tacke, F. and Arrese, M. and Chander Sharma, B. and Mostafa, I. and Bugianesi, E. and Wai-Sun Wong, V. and Yilmaz, Y. and George, J. and Fan, J. and Vos, M. B., Global Perspectives on Nonalcoholic Fatty Liver Disease and Nonalcoholic Steatohepatitis. *Hepatology*, 2019, 69, 2672-2682.
4. Fu, D.-f. and Chen, B., The relationship between the systemic immune inflammation index and the nonalcoholic fatty liver disease in American adolescents. *BMC Gastroenterology*, 2024, 24, 233.
5. Shi, J. and Chen, J. and Zhang, Z. and Qian, G., Multi-dimensional comparison of abdominal obesity indices and insulin resistance indicators for assessing NAFLD. *BMC Public Health*, 2024, 24.
6. Tang, M. and Cao, H. and Ma, Y. and Yao, S. and Wei, X. and Tan, Y. and Liu, F. and Peng, Y. and Fan, N., USP13 ameliorates nonalcoholic fatty liver disease through inhibiting the activation of TAK1. *J Transl Med*, 2024, 22, 671.
7. Lin, Z. and Huang, Z. and Qiu, J. and Shi, Y. and Zuo, D. and Qiu, Z. and He, W. and Niu, Y. and Yuan, Y. and Li, B., m(6)A-mediated lnc-OXAR promotes oxaliplatin resistance by enhancing Ku70 stability in non-alcoholic steatohepatitis-related hepatocellular carcinoma. *J Exp Clin Cancer Res*, 2024, 43, 206.
8. Sumida, Y. and Yoneda, M., Current and future pharmacological therapies for NAFLD/NASH. *J Gastroenterol*, 2018, 53, 362-376.
9. Chen, H. and Yan, S. and Xiang, Q. and Liang, J. and Deng, X. and He, W. and Cheng, Y. and Yang, L., Network analysis and experimental verification of Salvia miltiorrhiza Bunge-Reynoutria japonica Houtt. drug pair in the treatment of non-alcoholic fatty liver disease. *BMC Complementary Medicine and Therapies*, 2024, 24, 305.
10. Castillo, V. and Figueroa, F. and González-Pizarro, K. and Jopia, P. and Ibacache-Quiroga, C., Probiotics and Prebiotics as a Strategy for Non-Alcoholic Fatty Liver Disease, a Narrative Review. *Foods*, 2021, 10.
11. Fang, S. and Suh, J. M. and Reilly, S. M. and Yu, E. and Osborn, O. and Lackey, D. and Yoshihara, E. and Perino, A. and Jacinto, S. and Lukasheva, Y. and Atkins, A. R. and Khvat, A. and Schnabl, B. and Yu, R. T. and Brenner, D. A. and Coulter, S. and Liddle, C. and Schoonjans, K. and Olefsky, J. M. and Saltiel, A. R. and Downes, M. and Evans, R. M., Intestinal FXR agonism promotes adipose tissue browning and reduces obesity and insulin resistance. *Nat Med*, 2015, 21, 159-165.
12. Lee, Y. and Doumouras, A. G. and Yu, J. and Brar, K. and Banfield, L. and Gmora, S. and Anvari, M. and Hong, D., Complete Resolution of Nonalcoholic Fatty Liver Disease After Bariatric Surgery: A Systematic Review and Meta-analysis. *Clin Gastroenterol Hepatol*, 2019, 17, 1040-1060.e1011.
13. Kumar, S. and Mohanty, A. and Mantry, P. and Schwartz, R. E. and Haff, M. and Therapondos, G. and Noureddin, M. and Dieterich, D. and Girgrah, N. and Cohn, K. and Savanth, M. and Fuchs, M., Deploying a metabolic dysfunction-associated steatohepatitis consensus care pathway: findings from an educational pilot in three health systems. *BMC Prim Care*, 2024, 25, 265.
14. Madrigal Pharmaceuticals. Madrigal pharmaceuticals announces FDA approval of Rezdifra™ (resmetirom) for the treatment of patients with noncirrhotic nonalcoholic steatohepatitis (MASH) with moderate to advanced liver fbrosis. 2024. *https://ir.Madrigalpharma.com/news-releases/news-*

release-details/madrigal-pharmaceuticals-announces-fdaapproval-rezdifratm.
15. Gervois, P. and Torra, I. P. and Fruchart, J. C. and Staels, B., Regulation of lipid and lipoprotein metabolism by PPAR activators. *Clin Chem Lab Med*, 2000, 38, 3-11.
16. Erhardt, A. and Stahl, W. and Sies, H. and Lirussi, F. and Donner, A. and Häussinger, D., Plasma levels of vitamin E and carotenoids are decreased in patients with nonalcoholic steatohepatitis (NASH). *European Journal of Medical Research*, 2011, 16, 76.
17. Porcuna, J. and Mínguez-Martínez, J. and Ricote, M., The PPARα and PPARγ Epigenetic Landscape in Cancer and Immune and Metabolic Disorders. *Int J Mol Sci*, 2021, 22.
18. Xu, X. and Poulsen, K. L. and Wu, L. and Liu, S. and Miyata, T. and Song, Q. and Wei, Q. and Zhao, C. and Lin, C. and Yang, J., Targeted therapeutics and novel signaling pathways in non-alcohol-associated fatty liver/steatohepatitis (NAFL/NASH). *Signal Transduct Target Ther*, 2022, 7, 287.
19. Guan, Y., Peroxisome proliferator-activated receptor family and its relationship to renal complications of the metabolic syndrome. *J Am Soc Nephrol*, 2004, 15, 2801-2815.
20. Neuschwander-Tetri, B. A. and Loomba, R. and Sanyal, A. J. and Lavine, J. E. and Van Natta, M. L. and Abdelmalek, M. F. and Chalasani, N. and Dasarathy, S. and Diehl, A. M. and Hameed, B. and Kowdley, K. V. and McCullough, A. and Terrault, N. and Clark, J. M. and Tonascia, J. and Brunt, E. M. and Kleiner, D. E. and Doo, E., Farnesoid X nuclear receptor ligand obeticholic acid for non-cirrhotic, non-alcoholic steatohepatitis (FLINT): a multicentre, randomised, placebo-controlled trial. *Lancet*, 2015, 385, 956-965.
21. Cheng, H. S. and Tan, W. R. and Low, Z. S. and Marvalim, C. and Lee, J. Y. H. and Tan, N. S., Exploration and Development of PPAR Modulators in Health and Disease: An Update of Clinical Evidence. *Int J Mol Sci*, 2019, 20.
22. A. ClinicalTrials, Multicentre, randomized, double blind, placebo-controlled study to evaluate the efficacy and safety of GFT505 once daily on steatohepatitis in patients with non-alcoholic steatohepatitis (MASH).[EB/ OL], 07-14)[2019-06-18],*https://clinicaltrials.gov/ct2/show/NCT01694849?term=NCT0169 4849&rank =1, 2016.*
23. Staels, B. and Rubenstrunk, A. and Noel, B. and Rigou, G. and Delataille, P. and Millatt, L. J. and Baron, M. and Lucas, A. and Tailleux, A. and Hum, D. W. and Ratziu, V. and Cariou, B. and Hanf, R., Hepatoprotective effects of the dual peroxisome proliferator-activated receptor alpha/delta agonist, GFT505, in rodent models of nonalcoholic fatty liver disease/nonalcoholic steatohepatitis. *Hepatology*, 2013, 58, 1941-1952.
24. Cariou, B. and Zaïr, Y. and Staels, B. and Bruckert, E., Effects of the new dual PPAR α/δ agonist GFT505 on lipid and glucose homeostasis in abdominally obese patients with combined dyslipidemia or impaired glucose metabolism. *Diabetes Care*, 2011, 34, 2008-2014.
25. A. ClinicalTrials, Multicenter, Randomized, Double-Blind, Placebo-Controlled Phase III Study to Evaluate the Efficacy and Safety of Elafibranor in Patients with Nonalcoholic Steatohepatitis (MASH) and Fibrosis[EB/OL, 2019-04-01 [2019-06-18], *https://clinicaltrials.gov/ct2/show/NCT02704403.*
26. A.A. Idrus, Genfit's elafibranor en route to MASH graveyard with phase 3 flop[EB/ OL, 2020,05-11)[2020-06-17],*https://www.fiercebiotech.com/biotech/genfit-selafibranor-en-route-to-MASH-graveyard-phase-3-flop.*
27. Hou, W. and Xu, H., Incorporating Selenium into Heterocycles and Natural Products─From Chemical Properties to Pharmacological Activities. *Journal of Medicinal Chemistry*, 20 22,65,4436-4456.
28. He, H. and Huang, D. and Xie, P. and Dong, J. and Huo, S. and Li, S. and Ma, L. and Chen, T., Research progress on selenium system in cancer therapy: Focus on interface modifications and improvement of interactions. *Surfaces and Interfaces*, 2025, 5 6, 105642.
29. Chen, M. and Cao, W. and Wang, J. and Cai, F. and Zhu, L. and Ma, L. and Chen, T., Selenium Atom-Polarization Effect Determines TrxR-Specific Recognition of Metallodrugs. *Journal of the American Chemical Society*, 2022, 144, 20825-20833.
30. Liu, T. and Zeng, L. and Jiang, W. and Fu, Y. and Zheng, W. and Chen, T., Rational design of cancer-targeted selenium nanoparticles to antagonize multidrug resistance in cancer

cells. *Nanomedicine: Nanotechnology, Biology and Medicine,* 2015, 11, 947-958.
31. Andrade, R. J. and Chalasani, N. and Björnsson, E. S. and Suzuki, A. and Kullak-Ublick, G. A. and Watkins, P. B. and Devarbhavi, H. and Merz, M. and Lucena, M. I. and Kaplowitz, N. and Aithal, G. P., Drug-induced liver injury. *Nat Rev Dis Primers,* 2019, 5, 58.
32. Sviklāne, L. and Olmane, E. and Dzērve, Z. and Kupčs, K. and Pīrāgs, V. and Sokolovska, J., Fatty liver index and hepatic steatosis index for prediction of non-alcoholic fatty liver disease in type 1 diabetes. *J Gastroenterol Hepatol,* 2018, 33, 270-276.
33. Xiang, C. and Chen, X. and Yao, J. and Yang, N. and Yu, J. and Qiu, Q. and Zhang, S. and Kong, X. and Zhao, L. and Fan, Z.-C. and Yu, P. and Teng, Y.-o., Design, synthesis and anti-NASH effect evaluation of novel GFT505 derivatives in vitro and in vivo. *European Journal of Medicinal Chemistry,* 2023, 257, 115510.
34. Choi, A. M. and Ryter, S. W. and Levine, B., Autophagy in human health and disease. *N Engl J Med,* 2013, 368, 651-662.
35. Yang, D. and Wan, Y., Molecular determinants for the polarization of macrophage and osteoclast. *Semin Immunopathol,* 2019, 41, 551-563.
36. Kuzu, O. F. and Noory, M. A. and Robertson, G. P., The Role of Cholesterol in Cancer. *Cancer Res,* 2016, 76, 2063-2070.
37. Xiong, X. and Ren, Y. and Cui, Y. and Li, R. and Wang, C. and Zhang, Y., Obeticholic acid protects mice against lipopolysaccharide-induced liver injury and inflammation. *Biomed Pharmacother,* 2017, 96, 1292-1298.
38. Asgharpour, A. and Cazanave, S. C. and Pacana, T. and Seneshaw, M. and Vincent, R. and Banini, B. A. and Kumar, D. P. and Daita, K. and Min, H. K. and Mirshahi, F. and Bedossa, P. and Sun, X. and Hoshida, Y. and Koduru, S. V. and Contaifer, D., Jr. and Warncke, U. O. and Wijesinghe, D. S. and Sanyal, A. J., A diet-induced animal model of non-alcoholic fatty liver disease and hepatocellular cancer. *J Hepatol,* 2016,65,579-588.
39. Zou, Y. and Zhong, L. and Hu, C. and Zhong, M. and Peng, N. and Sheng, G., LDL/HDL cholesterol ratio is associated with new-onset NAFLD in Chinese non-obese people with normal lipids: a 5-year longitudinal cohort study. *Lipids Health Dis,* 2021, 20, 28.
40. Deprince, A. and Haas, J. T. and Staels, B., Dysregulated lipid metabolism links NAFLD to cardiovascular disease. *Mol Metab,* 2020, 42,101092.
41. Lin, X. L. and Zeng, Y. L. and Ning, J. and Cao, Z. and Bu, L. L. and Liao, W. J. and Zhang, Z. M. and Zhao, T. J. and Fu, R. G. and Yang, X. F. and Gong, Y. Z. and Lin, L. M. and Cao, D. L. and Zhang, C. P. and Liao, D. F. and Li, Y. M. and Zeng, J. G., Nicotinate-curcumin improves NASH by inhibiting the AKR1B10/ACCα-mediated triglyceride synthesis. *Lipids Health Dis,* 2024,23, 201.
42. Cobbina, E. and Akhlaghi, F., Non-alcoholic fatty liver disease (NAFLD) - pathogenesis, classification, and effect on drug metabolizing enzymes and transporters. *Drug Metab Rev,* 2017, 49, 197-211.
43. Lyu, S. and Cai, Z. and Yang, Q. and Liu, J. and Yu, Y. and Pan, F. and Zhang, T., Soybean meal peptide Gly-Thr-Tyr-Trp could protect mice from acute alcoholic liver damage: A study of protein-protein interaction and proteomic analysis. *Food Chem,* 2024, 451,139337.

Supplementary File Link